Digital Volume Correlation based on MRI: A novel methodology enabling measurements of the internal deformation and strain in human intervertebral discs during loading

S. Tavana[1a], J.N.Clark[1], N. Baxan[2], N. Newell[1], U. Hansen[1]

[1] Dept. of Mechanical Engineering, Imperial College London.
[2] Biomedical Imaging Centre, Dept. of Medicine, Imperial College London.

[a]S.tavana17@imperial.ac.uk

Introduction

Low back pain (LBP) is one of the main causes of musculoskeletal disorders and disabilities, and has an economic burden on governments and public health [1]. Seventy to eighty five percent of people experience LBP at some point in their lifetime [2]. Intervertebral disc (IVD) degeneration has been found to be associated with LBP [3]. The primary function of the IVD is mechanical, and degeneration is associated with loss of internal structural integrity and altered material properties [4], so quantifying the internal deformation and strain distributions within the IVD are crucial for understanding progressive mechanical change in degenerate discs, development and evaluation of treatment methods, and improving the effectiveness of spinal implant designs to restore the normal functions of the spine.

Micro CT has a great potential of visualizing microstructural patterns in bone, and digital volume correlation (DVC) based on micro CT has been widely used for strain measurement in trabecular and cortical bone [5]. Imaging of the IVD using high field strength MRI has shown microstructural patterns in the IVD (Figure 1). To date, no study has directly evaluated and compared the reliability of using different DVC approaches for strain measurement in soft tissues. DVC in combination with MRI may allow the internal 3D full field deformation and strain in human intervertebral discs (IVD) to be assessed; a possibility not offered by any current experimental methods. The aim of this study was to assess and compare the reliability of three DVC approaches for strain measurement in human IVDs.
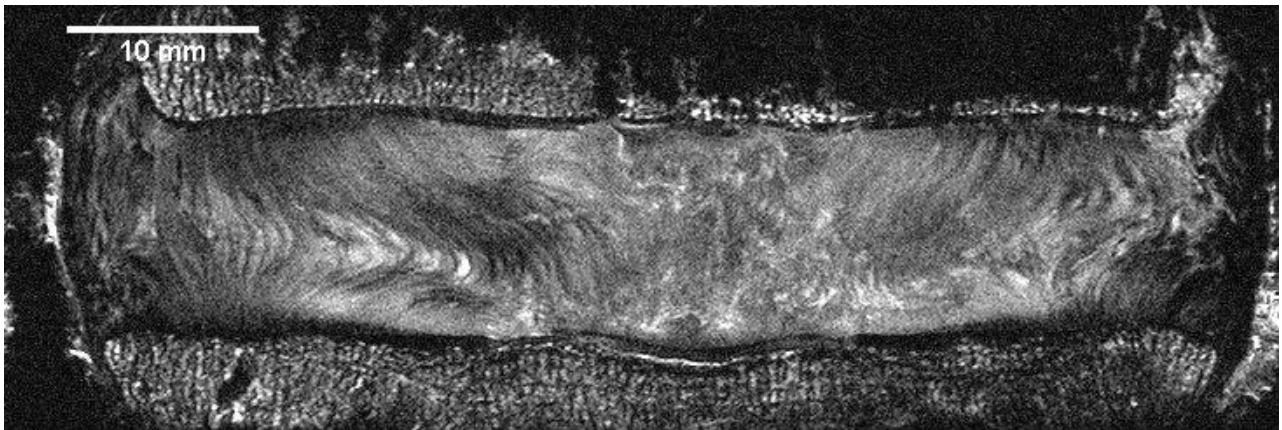

Fig.1 High field 9.4 T MRI machine was used in this study for visualizing microstructural patterns of IVDs. T_2 weighted MRI of a typical human IVD specimen is shown.

Methods

Eight human vertebral body – IVD – vertebral body specimens (L3-L4 and L4-L5, age = 55.5 ± 3.5 years (average ± SD), were used for this study. To enable samples to be imaged within a 9.4T MRI scanner, a custom made compression rig was designed to apply an axial compressive load to the sample. Two sets of images (with in plane resolution of (90 x 90) µm^2) were taken of each unloaded sample using exactly the same imaging protocol and without any sample repositioning between scans (zero-strain-study, Figure 2). Four samples were then loaded to 2 mm of displacement and reimaged using the same protocol (loaded-study, Figure 2). The following DVC approaches were used for different subset sizes in zero-strain-study:

fast-Fourier-transform (FFT), direct-correlation (DC), and a combination of both individual approaches (FFT+DC). The optimised setting was then used for strain calculation in the loaded samples.
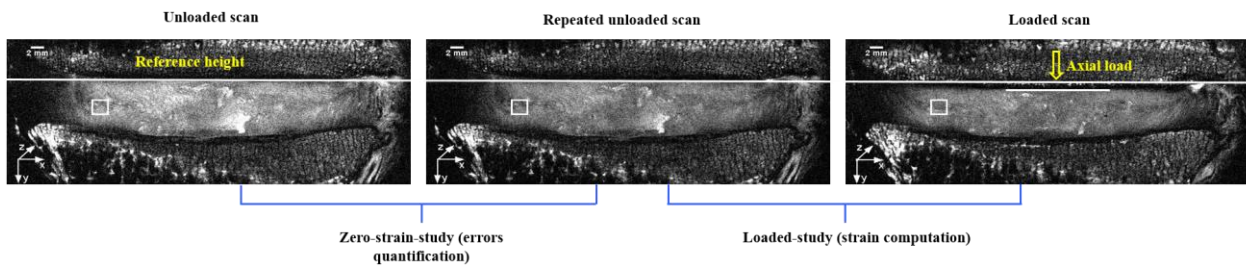

Fig. 2 Mid-coronal planes of the typical IVD are shown in unloaded (left), repeated unloaded (middle), and loaded (right) situation. Unloaded scans and repeated unloaded scans were used for calculating DVC errors (zero-strain-study), and the unloaded scan and the loaded scan were used for calculating strain distribution throughout IVD (loaded-study). Sample height are also shown in the initial state and after 2mm compression. The white square indicates the subset size that used for the loaded study (56 voxels and 50% overlap, equivalent to 2.52 mm).

Finally, for validating MRI_DVC performance manual segmentation was used to calculate the changes in height. The disc heights were measured in mid-coronal planes in the unloaded and loaded images. Then, axial strains were calculated by dividing the difference between the heights of the IVD before and after applying load by initial height (ImageJ 1.49u, National Health Institute, USA).
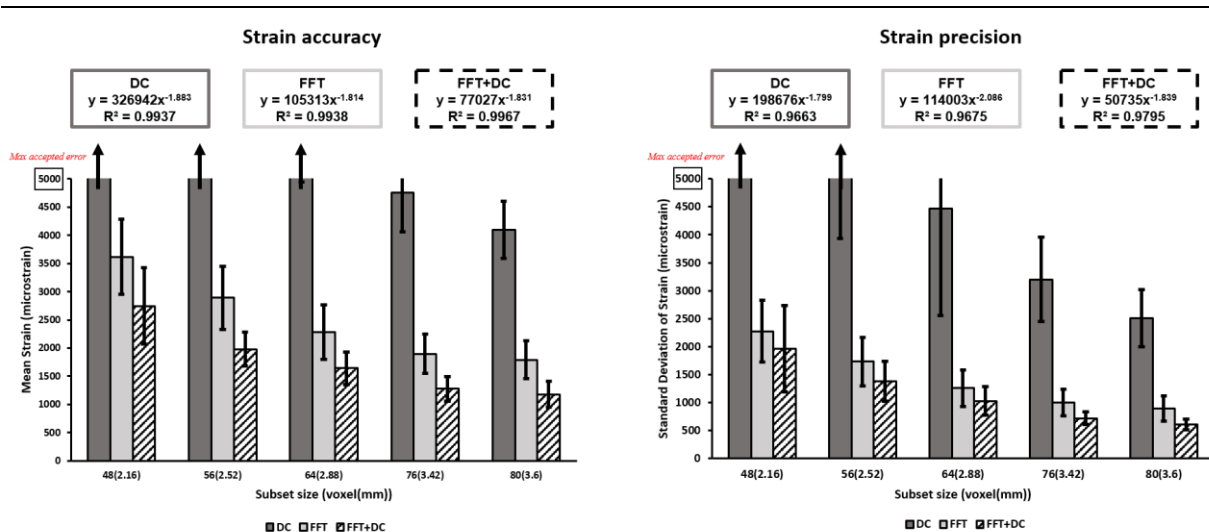

Fig. 3 Strain accuracy (left) and precision (right) for three DVC approaches. For better interpretation of the results, trend of strain accuracy and precision as a function of spatial resolution were only shown for the subset sizes range from 48 to 80 voxels. The trendline (power-law) equations and R-squared are reported for all three approaches for the full range (8 to 88 voxel). The scales on the graphs were limited to the maximum accepted error.

Results

For all three approaches, both strain accuracy and precision improved steadily with increasing subset size, following a power-law relationship with coefficient of determination (R^2) greater than 0.96 (Figures 3). For all subset sizes both accuracy and precision (Figure 3) were higher ($p<0.005$) for the FFT+DC approach (at best: 1070±226 and 636±206 µs, respectively), and the FFT approach (at best: 1587±381 and 847±184 µs, respectively), than those of the DC approach (at best: 3403±611 and 2170±539 µs, respectively). For the scope of this study, the maximum accepted measurement error was determined as 5000 microstrain, which

is less than 10% of the magnitude of the strain in the loaded IVDs in this study. A complementary validation test was conducted on the loaded samples by comparing the axial strain (Eyy) calculated by the DVC-MRI method, against the axial strain measured manually. There was a linear correlation between manual and DVC-MRI measurement of axial strain (r^2=0.98, p≤0.01, Figure 4).
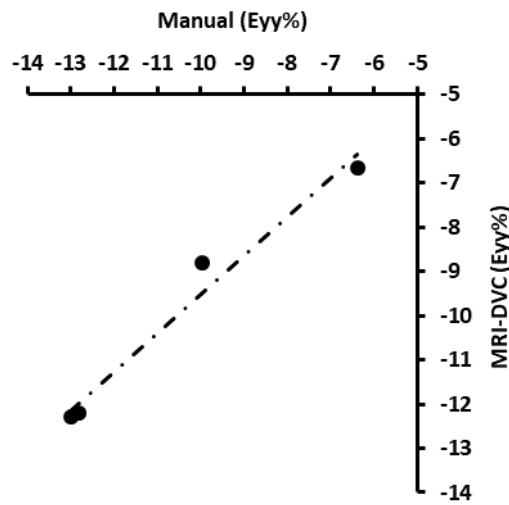

Fig. 4 MRI-DVC strains calculated along the y direction demonstrated strong agreement with manual measurements of axial strain (r^2=0.98, p≤0.01).

Based on the accuracy and precision of different DVC approaches, the FFT+DC approach with subset size of 56 voxels and 50% overlap was used for the loaded study. Strain patterns of Exx (radial strain), Eyy (axial strain), and Exy (shear strain) are shown for mid-coronal plane of two IVDs. The radial strains along the x-direction were observed as vertical bands of compression and tension, the axial strains were compressive and large along a horizontal band at the mid-disc height and shear strains were highest close to the endplates (Figure 6, arrows).
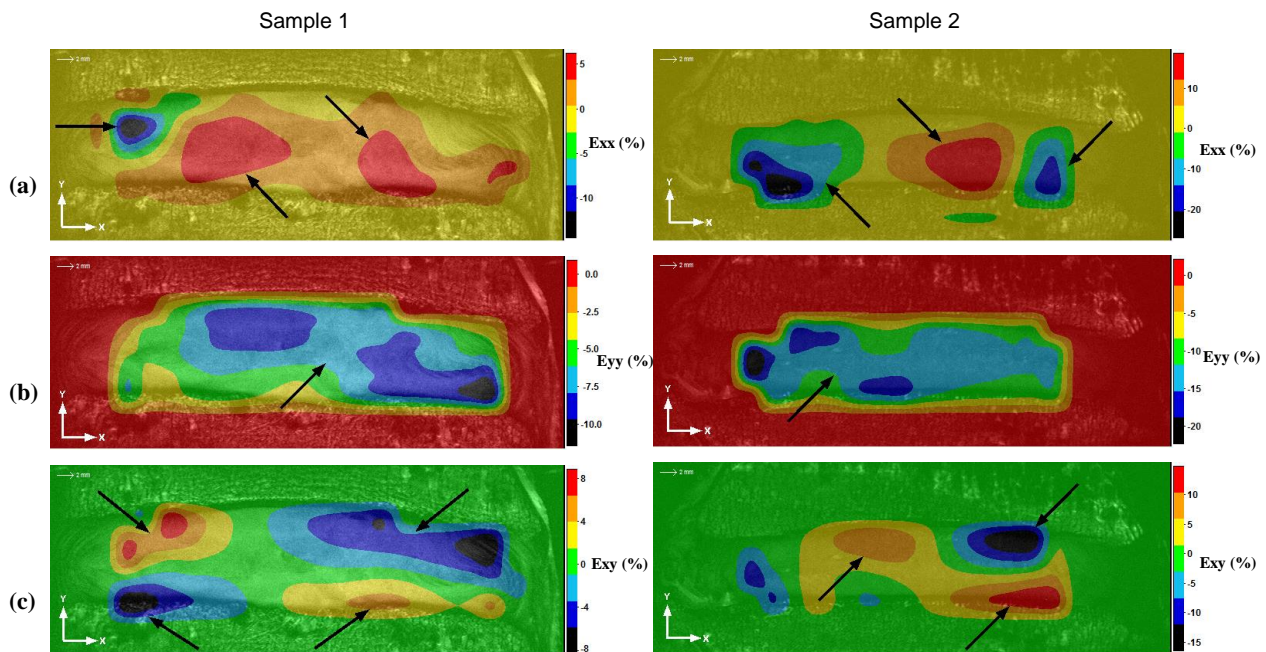

Fig. 2 (a) Radial (Exx), (b) axial (Eyy), and (c) shear (Exy) strain maps of two typical samples are shown, with strains reported as a percentage. Note that zero strain location in scale bar changes for each image, and features described in the text are denoted by black arrows.

Discussion

High field MRI has a unique potential for visualizing the internal structure of the IVD at the microstructural level without dissection and altering integrity of the disc [6]. The use of high field MRI with DVC allows the possibility of measuring internal strain of IVDs at the organ level. By taking into consideration both accuracy and precision, the FFT+DC method demonstrated the best performance. Errors in this approach did not exceed three percent of the average of all components of strain under 2mm compression load. Although the larger subset sizes can increase the reliability of the MRI-DVC, there is an inverse relationship between subset size and spatial resolution. As a result, the effect of increasing subset size on the spatial resolution should be considered. The strain patterns in the x-y plane of the loaded situation observed in this study demonstrate strong agreement with previous 2D strain analysis on IVDs [7]. Furthermore, the large shear strain observed at the endplates corresponded to strains predicted using finite element modelling [8]. In summary, the DVC-MRI method has unique potential for measuring the internal 3D deformations in the IVDs, and can conceivably be extended to the assessment of IVD deformation in patients.

References

[1]   Hoy, D., et al. Ann Rheum Dis, 2014. **73**: p. 968-974.
[2]   Andersson, G.B.J. The Lancet, 1999. **354**(9178): p. 581-585.
[3]   Luoma, K., et al. Spine, 2000. **25**(4): p. 487-492.
[4]   Adams, M.A. and P.J. Roughley, Spine, 2006. **31**(18): p. 2151-2161.
[5]   Roberts, B.C.et al. J Biomech, 2014. **47**(5): p. 923-34.
[6]   Sharabi, M., et al. Spine Journal, 2018. **18**(11): p. 2119-2127.
[7]   O'Connell, G.D., et al., Spine (Phila Pa 1976), 2007. **32**(25): p. 2860-8.
[8]   Eberlein, R.et al, CMBBE, 2001. **4**(3): p. 209-229.